This article has been accepted for publication in a future issue of this journal, but has not been fully edited. Content may change prior to final publication. Citation information: DOI 10.1109/TAES.2017.2735118, IEEE Transactions on Aerospace and Electronic Systems

Computationally Efficient TDOA/FDOA Estimation for Unknown Communication Signals in Electronic Warfare Systems

Dong-Gyu Kim, Geun-Ho Park, Jin-Oh Park, Young-Mi Park, Wook-Hyeon Shin, and *Hyoung-Nam Kim*, *Member, IEEE*

***Abstract*—The cross ambiguity function (CAF) has been commonly used to find time difference of arrival (TDOA) and frequency difference of arrival (FDOA). In most cases, direct computation of the CAF by using a conventional method, such as fast Fourier transform, is too computationally intensive. Thus, a two-stage approach consisting of a coarse mode to find rough TDOA/FDOA estimates and a fine mode for precise estimation was introduced. However, there has been no methodology for selecting an interpolation factor determined by the sampling frequency and target resolution which significantly affects the computational complexity. In addition, even if the computational complexity can be reduced by using the optimal interpolation factor, the huge transmission data through the datalink between sensors and the central station still remains to be an obstacle for an electronic warfare (EW) system. In this respect, we derive an optimal interpolation factor and then propose a new two-stage TDOA/FDOA estimation algorithm using a resampling block to reduce the computational complexity and the data size simultaneously in EW systems. In the proposed method the optimal interpolation factor can be used irrespective of the sampling frequency and the target resolution. Simulation results show that the optimal interpolation factor reduces the computational burden without the loss of estimation performance.**

***Index Terms*— TDOA, FDOA, electronic warfare, cross ambiguity function.**

I. Introduction

In electronic warfare (EW) systems, estimating the source location of non-cooperative signals is quite important for surveillance and planning military strategies. Since there is usually no preliminary information about the non-cooperative signals, such as the amplitude, frequency, and modulation method, such emitter information must first be extracted from only the intercepted signals. Then, the emitter information is used to estimate primary observations such as the direction of arrival (DOA), time difference of arrival (TDOA), and frequency difference of arrival (FDOA) [1].

In recent years, TDOA and FDOA have received much attention due to the possibility of better estimation performance [1-6]. TDOA/FDOA localization generally consists of two parts. First we need to estimate the TDOA and FDOA of the intercepted signals [7-13]. Then this information is used via solving the appropriate set of non-linear equations [1-4]. This paper is focused on the problem of computationally efficient estimation of TDOA and FDOA.

D.-G. Kim, G.-H. Park, and H.-N Kim are with the Department of Electronics Engineering, Pusan National University, Busan 46241, Republic of Korea (e-mail: hnkim@pusan.ac.kr); J.-O. Park is with LIG Nex1, Seongnam, Republick of Korea; Y.-M. Park and W.-H Shin are with Agency for Defense Development, Daejeon 34186, Korea

Let $r_1(t)$ and $r_2(t)$ be intercepted signals at two moving sensors located far apart from each other. The signals are time-shifted and frequency-shifted from a radiated signal of an unknown emitter $s(t)$ and given by [14]:

$$\begin{aligned} r_1(t) &= s(t-\tau_1)e^{j2\pi v_1 t} + n_1(t), \quad 0 \le t < T \\ r_2(t) &= s(t-\tau_2)e^{j2\pi v_2 t} + n_2(t), \quad 0 \le t < T \end{aligned} \tag{1}$$

where T is the collection time, τ_1 and τ_2 are time delays between the emitter and each sensor, v_1 and v_2 are Doppler frequencies caused by the movement of each sensor, and $n_1(t)$ and $n_2(t)$ are additive white Gaussian noise at each sensor. Since these two sensors are far away from each other, a datalink between each sensor is needed to estimate TDOA and FDOA from the two intercepted signals. Two sensors transfer their intercepted data to a central processor through the datalink, which may take a long time for a large amount of data. This communication scenario is not suitable for EW systems, where the important index of evaluation is the speed of data processing. The data size to be handled depends on the characteristics of the signal, such as bandwidth and center frequency. This size affects the selection of the TDOA/FDOA estimation algorithm [15].

When a pulse train signal is received from radar, the size of the overall sampled data is too large to transfer to the other sensor or the central processor within a limited time because the pulse train signal is wideband signal. In order to represent the original signal by a discrete-time signal without loss of information, the sampling rate has to be two times larger than the bandwidth. Thus, only information about the receiving time at each sensor is usually transferred instead of all pulse data. TDOA can be acquired by just computing the difference between the receiving times of each sensor [5]. Similarly, FDOA can be obtained from the difference of Doppler frequencies between each sensor [16, 17].

On the other hand, communication signals or narrowband signals can be sampled with a low sampling frequency. Thus, all sampled data can be transferred via datalink for TDOA/FDOA estimation. To estimate TDOA and FDOA between two collected signals, the signal received at one sensor is transmitted to the other sensor. Then, the collected signals are used to find the cross ambiguity function (CAF) [14]:

This article has been accepted for publication in a future issue of this journal, but has not been fully edited. Content may change prior to final publication. Citation information: DOI 10.1109/TAES.2017.2735118, IEEE Transactions on Aerospace and Electronic Systems

$$A(\tau, \nu) = \int_{-\infty}^{\infty} r_1(t) r_2^*(t+\tau) e^{j2\pi\nu t} dt \,, \tag{2}$$

where τ and v stand for the time difference and the Doppler-frequency difference, respectively. Since $|A(\tau, v)|$ is maximum at $(\tau, v) = (\tau_2-\tau_1, v_2-v_1)$, TDOA and FDOA can be estimated by finding where the CAF is maximum.

There have been several conventional TDOA/FDOA estimation methods based on CAF, some of which have used higher-order statistics [7], wideband signals [8], uncorrelated signals [9], and CAF-MAP [10]. These methods were developed to enhance the accuracy in special cases. Efficient computation of CAF has been studied because CAF requires computing correlation values on two-dimensional axes of τ and v [6, 11]. The use of FFT or decimation in time can reduce the computations on the axis of the frequency difference v, and thus makes it possible for CAF to be used in real applications. However, when a non-cooperative signal source is more than dozens of kilometers away from the sensors in EW, time resolution of dozens of nanoseconds should be secured to estimate the position of the emitter accurately. Hence, interpolation is needed to obtain the desired TDOA accuracy.

It is therefore not easy to achieve the aforementioned goals of high resolution and wide range in EW systems with only these kinds of conventional methods because of the increased computational burden. This burden is caused by the interpolated received signal for high resolution and the large number of points calculated for wide range, and the enormous amount of the computations cannot be implemented. To cope with this computational problem, a two-stage approach that coarsely finds a target point (coarse mode) and then finely searches for accurate TDOA and FDOA in the neighborhood of the point (fine mode) was presented [6, 12, 13].

In the coarse mode of determining a rough target point, CAF values are sparsely calculated without interpolation in a broad region, and then two-axis values corresponding to a maximum CAF value are determined as rough TDOA and FDOA estimates. To estimate TDOA and FDOA with fine resolution, the two received signals are interpolated in the second stage to achieve the desired time resolution [13]. So, CAF values are calculated at many sparse points in a wide region with few operations at each point obtained from the original received signals in the coarse mode. At a few dense points near the coarse estimates, CAF values are calculated with a large amount of operations at each point obtained from the interpolated signals. As a result, the computational complexity of the two-stage method varies with the number of points to be calculated in the fine mode, because the operations in the coarse mode are fixed by the sampling frequency of the original received signal. Thus, when the target resolution is fixed, the number of points in the fine mode is determined by the number of points in the coarse mode because the target resolution is directly related to the sample duration of the interpolated signal. Consequently, it is impossible to reduce the computational complexity when the desired target resolution is fixed because the numbers of points to be calculated in the coarse and fine modes are fixed in the conventional two-stage TDOA/FDOA estimation algorithm.

However, the computational complexity can be reduced by adding a resampling block using interpolation and decimation. When the number of points in the coarse mode is increased by a resampled signal, the number of points in the fine mode may be decreased. Thus, the overall computational complexity can be significantly reduced by designing the TDOA/FDOA estimation algorithm using the proposed resampling block. Also, it is possible to reduce the time required to transfer the received data from sensors to the central processor if a sampling frequency can be changed by a resampling block. In this sense, we derive an optimal interpolation factor related to the number of points to be calculated in the first and second stage and achieve the minimum computational complexity. In addition, we propose a reduced-complexity TDOA/FDOA estimation algorithm by adding a resampling block for using the optimal interpolation factor to reduce the computational complexity and the time for datalink simultaneously.

This paper is organized as follows. In Section II, we derive an optimal interpolation factor for the minimum operations of a two-stage method. Section III addresses the main details of the proposed TDOA/FDOA estimation scheme for minimizing computational burden and the time required for the datalink using the optimal interpolation factor according to control parameters like the distance between sensors. Section IV presents the results of the performance analysis using a newly-defined efficiency factor, and Section V concludes the paper.

II. Optimal Interpolation Factor for A Two-stage Method

The computational efficiency for TDOA/FDOA estimation can be enhanced by using a two-stage method consisting of a coarse mode for obtaining an initial value of the next stage and a fine mode for estimating an accurate value. In the coarse stage Stein's algorithm can be used. This method is known for efficient computation in the frequency band by exploiting a modified equation for implementing the CAF [14]. A discrete version of (2) can be divided into K_1 blocks, each of which includes L_1 samples [11], [14]:

$$A_{1st}(m_1, p_1) = \sum_{k_1=0}^{K_1-1} \sum_{l_1=0}^{L_1-1} b_{1,m_1}[k_1 L_1 + l_1] \exp\left(-j2\pi \frac{k_1 p_1}{K_1}\right) \tag{3}$$
$$\text{for } -\frac{M_1}{2} \le m_1 \le \frac{M_1}{2}, \; -\frac{f_{s1}}{2} \le p_1 \le \frac{f_{s1}}{2}$$

where f_{s1} is the sampling frequency and $b_{1,ml}[k_1L_1+l_1]$ is defined by:

This article has been accepted for publication in a future issue of this journal, but has not been fully edited. Content may change prior to final publication. Citation information: DOI 10.1109/TAES.2017.2735118, IEEE Transactions on Aerospace and Electronic Systems

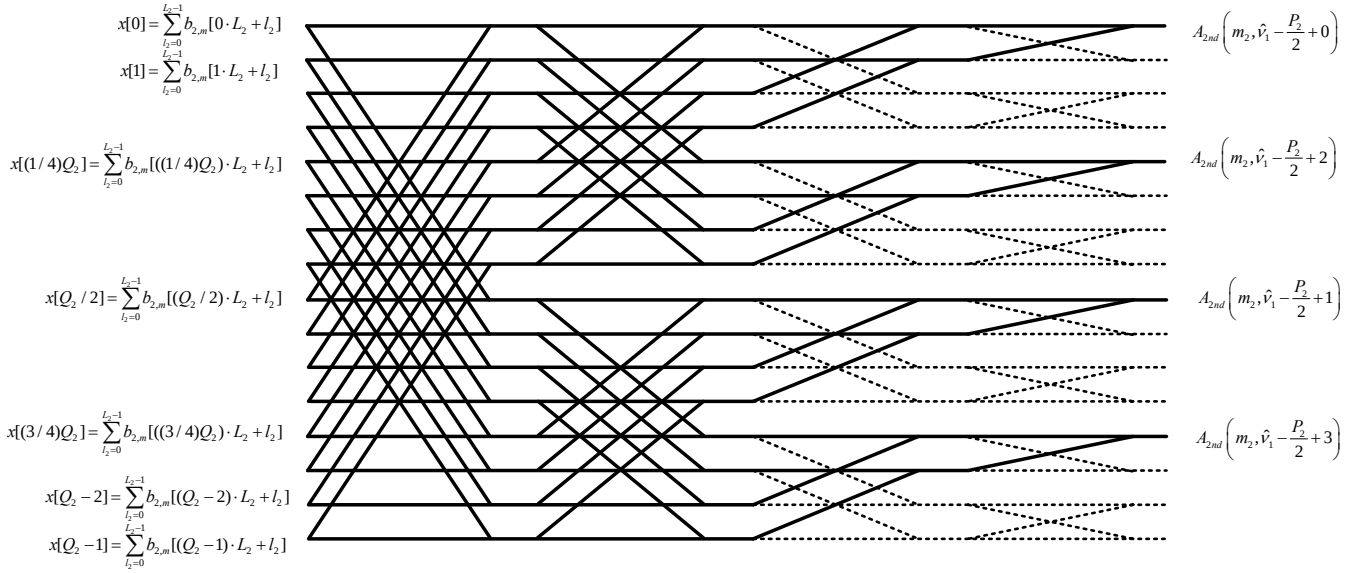

Fig. 1. Flow graph of FFT in second stage of proposed algorithm based on Skinner's pruned FFT.

$$b_{1,m_1}[n_1]=\begin{cases} r_1[n_1]r_2^*[n_1+m_1] & \text{for } 0\le n_1\le N_1-1,\\ 0 & \text{for } n_1\le -m_1,\ n_1\ge N_1-m_1,\end{cases} \quad (4)$$
$$n_1=k_1L_1+l_1 \text{ for } N_1\gg m_1,$$

Here, $r_1[n]$ and $r_2[n]$ are sampled signals from $r_1(t)$ and $r_2(t)$, respectively. N_1 is the number of samples of $r_1[n]$ and $r_2[n]$. The discrete-time CAF in (2) can be computed using a fast Fourier transform (FFT) with input of Q_1 samples composed of K_1 summed values of L_1 samples obtained by (4) and $(Q_1- K_1)$ zeros by zero padding. In this case, each input sample of the FFT except for padded zeros is calculated with L_1 complex multiplications and (L_1-1) complex additions.

Since we need to evaluate $b_{1,m1}[n]$ at all K_1 values, the number of computations required to obtain input data for FFT becomes K_1L_1 complex multiplications and $K_1(L_1\text{-}1)$ complex additions. Consequently, $A_{1st}(m_1, p_1)$ must be computed by a Q_1-length FFT for different M_1 values of m_1, and thus, the number of total operations in the coarse mode based on CAF using (3) becomes $M_1(Q_1\log_2Q_1+K_1L_1)$ complex multiplications and $M_1(Q_1\log_2Q_1+K_1(L_1\text{-}1))$ complex additions. One complex multiplication consists of four real multiplications and two real additions, while adding two complex numbers requires two real additions. Thus, the number of total operations is $M_1(4Q_1\log_2Q_1+4K_1L_1)$ real multiplications and $M_1\{4Q_1\log_2Q_1+K_1(4L_1\text{-}2)\}$ real additions.

In the second stage, fine estimates should be found based on the coarse estimation results obtained in the first stage. Letting $\hat{\tau}_1$ and $\hat{\upsilon}_1$ be the coarse estimates for TDOA and FDOA, respectively, the CAF based on the Stein's algorithm in the second stage is given by:

$$A_{2nd}(m_2,p_2)=\sum_{k_2=0}^{K_2-1}\sum_{l_2=0}^{L_2-1} b_{2,m_2}[k_2L_2+l_2]\exp\left(-j2\pi\frac{k_2p_2}{K_2}\right) \quad (5)$$
$$\text{for } \hat{\tau}_1-\frac{M_2}{2}\le m_2<\hat{\tau}_1+\frac{M_2}{2},\ -\frac{f_{s2}}{2L_2}\le p_2\le\frac{f_{s2}}{2L_2}$$

where f_{s2} is the resampling frequency of interpolated samples in the second stage, M_2 is the number of samples in the candidate range of a fine TDOA estimate, and $b_{2,m2}[k_2L_2+l_2]$ is defined by:

$$b_{2,m_2}[n_2]=\begin{cases} d_1[n_1]d_2^*[n_2+m_2] & \text{for } 0\le n_2\le N_2-1,\\ 0 & \text{for } n_2\le -m_2,\ n_2\ge N_2-m_2,\end{cases}$$
$$n_2=k_2L_2+l_2 \text{ for } N_2\gg m_2, \quad (6)$$

where $d_1[n_1]$ and $d_2[n_2]$ are interpolated sequences of $r_1[n_1]$ and $r_2[n_2]$, respectively. N_2 is the number of samples of interpolated sequences.

Similarly to the first stage, the number of total operations of (5) can be calculated as $M_2(4Q_2\log_2Q_2+4K_2L_2)$ real multiplications and $M_2\{4Q_2\log_2Q_2+2K_2(L_2\text{-}1)\}$ real additions. However, Stein's method may not be efficient for searching for a fine FDOA because it calculates CAF values at all frequencies in the full FFT range, which is determined by a new sampling frequency obtained from an interpolation factor and a grouping parameter L_2 without any use of a coarse FDOA estimate. In order to reduce the computational operations in searching for a fine FDOA, we need to focus on the neighborhood of the coarse FDOA estimate. The direct method (also called the brute force method or summation method) in [11], [13] and the pruned FFT method in [18] are known to be suitable in terms of computational burden for cases of only a narrow spectrum of interest. The pruned FFT is preferable over the direct method due to its lower complexity. Thus, we incorporate the pruned FFT into Stein's algorithm as follows:

This article has been accepted for publication in a future issue of this journal, but has not been fully edited. Content may change prior to final publication. Citation information: DOI 10.1109/TAES.2017.2735118, IEEE Transactions on Aerospace and Electronic Systems

TABLE I
THE NUMBER OF REQUIRED OPERATIONS

Method	Real multiplication	Real addition
Brute-force Method[13]	$4M_2Q_2N_2$	$2M_2Q_2N_2$
FFT[13]	$M_2(4rN_2\log_2(rN_2)+4N_2)$	$M_2(4rN_2\log_2(rN_2)+2N_2)$
Stein's Algorithm[14]	$M_2(4Q_2\log_2Q_2+4N_2)$	$M_2(4Q_2\log_2Q_2+4N_2-2K_2)$
Pruned FFT[18]	$M_2(2rN_2\log_2(P_2)+4N_2)$	$M_2(3rN_2\log_2(P_2)$ $+2rN_2-2P_2+2N_2)$
Stein's algorithm +Pruned FFT	$M_2(2Q_2\log_2P_2+4N_2)$	$M_2(3Q_2\log_2(P_2)+2Q_2$ $-2P_2+4N_2-2K_2)$

$$A_{2nd}(m_2,p_2)=\sum_{k_2=0}^{K_2-1}\sum_{l_2=0}^{L_2-1}b_{2,m}[k_2L_2+l_2]\exp\left(-j2\pi\frac{k_2p_2}{K_2}\right) \quad (7)$$

$$\text{for}\quad \hat{\tau}_1-\frac{M_2}{2}\le m_2<\hat{\tau}_1+\frac{M_2}{2},\ \hat{v}_1-\frac{P_2}{2}\le p_2<\hat{v}_1+\frac{P_2}{2}$$

where m_2 is a time shift index, p_2 is a frequency shift index, and P_2 is the number of points of interest among all the output points of FFT. As shown in Fig. 1, only P_2 points in the neighborhood of the coarse FDOA estimate are calculated by the solid butterfly lines. By multiplying the twiddle factor, it is possible to obtain CAF values at the points of interest corresponding to the frequency indices of FFT near the coarse estimate.

Consequently, the pruned-FFT-based Stein's algorithm requires $M_2(2Q_2\log_2(P_2)+4N_2)$ real multiplications and $M_2(3Q_2\log_2(P_2)+2Q_2-2P_2+4N_2-2K_2)$ real additions. The computational complexity of some methods is given in Table I, including the pruned-FFT-based Stein's algorithm. We introduce a proportional coefficient r that satisfies the relation of $Q_2=rK_2$ to compare the computational complexities of several methods to achieve the same frequency-domain sampling interval.

When we calculate the fine estimates, we use only M_2 points near the coarse estimates, as shown in Fig. 2. If each sensor is fixed, the range of TDOA values is also fixed. Thus, M_2 is related to M_1 as follows:

$$M_1M_2=M\ , \quad (8)$$

where M is a constant value set by the interesting range of TDOAs as follows:

$$M=\left\lceil\frac{Rf_{s2}}{c}\right\rceil \quad (9)$$

where $\lceil\cdot\rceil$ stands for the smallest following integer, R denotes the distance between each sensor, and c is a propagation velocity.

Now, the number of overall operations in the first and second stages can be obtained by:

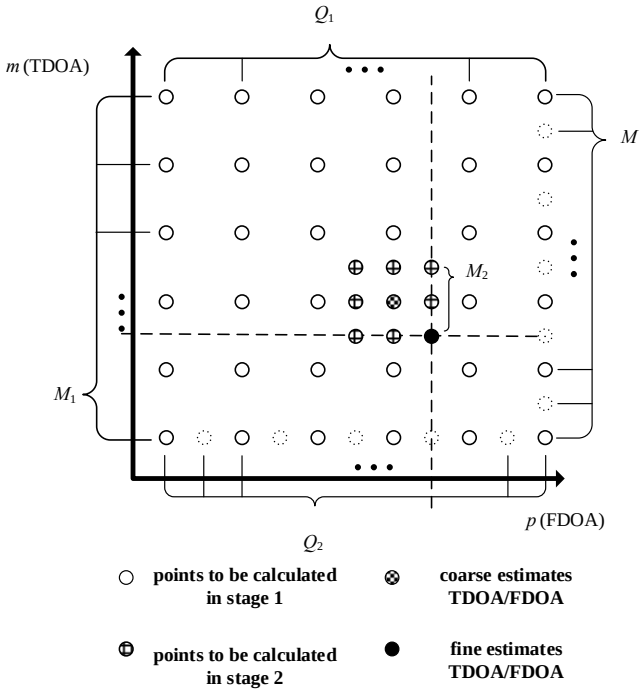

Fig. 2. Description of the number of points to be calculated in stage 1 and stage 2.

$$\begin{aligned}NC=&M_1(8Q_1\log_2Q_1+8N_1-2K_1)\\&+M_2(5Q_2\log_2P_2+8N_2+2Q_2-2P_2-2K_2),\end{aligned} \quad (10)$$

where K_1 is determined by:

$$K_1=\frac{N_1}{L_1}=\frac{f_{s2}T}{M_2L_1}. \quad (11)$$

Here L_1 is obtained by

$$L_1=\left\lfloor\frac{f_{s2}}{M_2v_{mm}}\right\rfloor, \quad (12)$$

where $\lfloor\cdot\rfloor$ is the largest previous integer and v_{mm} is a difference between minimum and maximum FDOAs to be considered in the system. Similarly, K_2 and L_2 are determined as follows:

$$K_2=\frac{N_2}{L_2}=\frac{f_{s2}T}{L_2},\ L_2=\left\lfloor\frac{f_{s2}}{v_{mm}}\right\rfloor. \quad (13)$$

By approximating L_1 and L_2 without the use of the operator $\lfloor\cdot\rfloor$ and using (8), (11), and (13), (10) can be re-written by:

This article has been accepted for publication in a future issue of this journal, but has not been fully edited. Content may change prior to final publication. Citation information: DOI 10.1109/TAES.2017.2735118, IEEE Transactions on Aerospace and Electronic Systems

$$NC = \frac{M}{M_2}\left(8r_1 T v_{mm}\log_2\left(r_1 T v_{mm}\right) + 8\frac{f_{s2}}{M_2}T - 2Tv_{mm}\right) \quad (14)$$
$$M_2\left(r_2 T v_{mm}(5\log_2 P_2 + 2) + 8f_{s2}T - 2P_2 - 2Tv_{mm}\right)$$

Since most parameters except for M_2 are fixed in our design, if a target resolution is given we can find the optimal value of M_2 to minimize the number of computations by deriving the derivative of (14) with respect to M_2 as follows:

$$\begin{aligned}\frac{\partial}{\partial M_2}(NC) &= -16Mf_{s2}T\frac{1}{M_2^3} \\ &\quad - 2MTv_{mm}(4r_1\log_2(r_1Tv_{mm}) + 1)\frac{1}{M_2^2} \\ &\quad + \left(r_2 T v_{mm}(5\log_2 P_2 + 2) + 8f_{s2}T - 2P_2 - 2Tv_{mm}\right)\end{aligned} \quad (15)$$

By setting (15) to zero, we obtain a third-order fractional equation with a variable M_2:

$$-a\frac{1}{M_2^3} - b\frac{1}{M_2^2} + c = 0 \text{ for } a > 0,\ b > 0,\ c > 0, \quad (16)$$

where

$$a = 16Mf_{s2}T, \quad b = 2MTv_{mm}(4r_1\log_2(r_1Tv_{mm}) + 1),$$
$$c = r_2 T v_{mm}(5\log_2 P_2 + 2) + 8f_{s2}T - 2P_2 - 2Tv_{mm}.$$

Consequently, the optimal value of M_2 can be obtained by solving (16) using the root of a cubic equation:

$$\begin{aligned}M_2 &= \left[\frac{x_+ + x_-}{6c}\right]_{round}, \\ x_+ &= \sqrt[3]{36c(3ac + \sqrt{D})}, \quad x_- = \sqrt[3]{36c(3ac - \sqrt{D})} \\ D &= (3ac)^2 - \frac{4}{3}(b^3 c)\end{aligned} \quad (17)$$

where $[x]_{round}$ is an integer that is closest to x. Note that M_2 is also an interpolation factor referring to Fig. 2. The use of the optimal value of M_2 obtained from (17) guarantees the minimized computational burden for estimating fine TDOA and FDOA.

III. Two-stage TDOA/FDOA Estimation Using a Resampling Block

In this section, we propose an efficient two-stage TDOA/FDOA estimation algorithm by adding a resampling block using the optimal interpolation factor based on unknown received signals. To satisfy Nyquist sampling theory, the sampling rate has to be as large as possible at each sensor due to the lack of information about the bandwidth for the unknown intercepted signals. The data size of the intercepted signals with this high sampling rate is too large to transfer to another sensor or central processing unit in a limited amount of time. Thus, signal compression is needed to reduce the data size. To adjust the compression procedure, the bandwidth of the unknown signal has to be estimated using the root mean square (RMS) bandwidth, which is a part of the Cramer-Rao lower bound (CRLB) for TDOA [14, 19, 20]. The RMS bandwidth is defined by:

$$B_{rms} = \sqrt{\frac{\int_{-\infty}^{\infty} f^2 |S(f)|^2 df}{\int_{-\infty}^{\infty} |S(f)|^2 df}}, \quad (18)$$

where $S(f)$ is the Fourier transform of the unknown intercepted signal. Assuming that intercepted signals are band-limited unknown communication signals with the use of pulse shaping of a sinc signal, the spectrum of the intercepted signal has a rectangular form such that the RMS bandwidth is related to the signal bandwidth B_u as follows:

$$B_u \cong 2\sqrt{3}B_{rms}. \quad (19)$$

Sampled data of the intercepted signals with a high sampling rate are processed using an interpolator and a decimator to make the sampling rate as small as possible while satisfying Nyquist sampling theory based on the estimated bandwidth of the signal acquired from (19). The interval time for the datalink can be minimized by the reduced size of the data caused by the changed sampling frequency.

When a central processor receives the intercepted signal, it has to consider parameters such as the search range and velocity. First, to estimate the position of an emitter that is farther from the sensors, we have to increase the distance between each sensor [21]. However, this requires considering more points M in accordance with (9). Thus, we need to set a proper distance between each sensor by simultaneously considering the two conflicting objectives of low computational complexity and effective searching range.

When the unknown emitter moves at a certain velocity and several sensors are fixed, the difference between minimum and maximum FDOAs is determined by:

$$v_D = v_{MAX} - v_{MIN} = \left(f_c\frac{v}{c}\right) - \left(-f_c\frac{v}{c}\right) = 2f_c\frac{v}{c}, \quad (20)$$

where f_c is an unknown maximum carrier frequency and v is the expected maximum velocity of an emitter. We can determine the optimal values of M_1 and M_2 from the root of the cubic equation (17) derived in Section II after we choose the values of several parameters: v_D, M, the collection time T, the time resolution in the final stage $1/f_{s2}$, the frequency-domain sampling interval factors on the first stage r_1 and the second stage r_2, and the number of points P_2 to be calculated by pruned FFT.

This article has been accepted for publication in a future issue of this journal, but has not been fully edited. Content may change prior to final publication. Citation information: DOI 10.1109/TAES.2017.2735118, IEEE Transactions on Aerospace and Electronic Systems

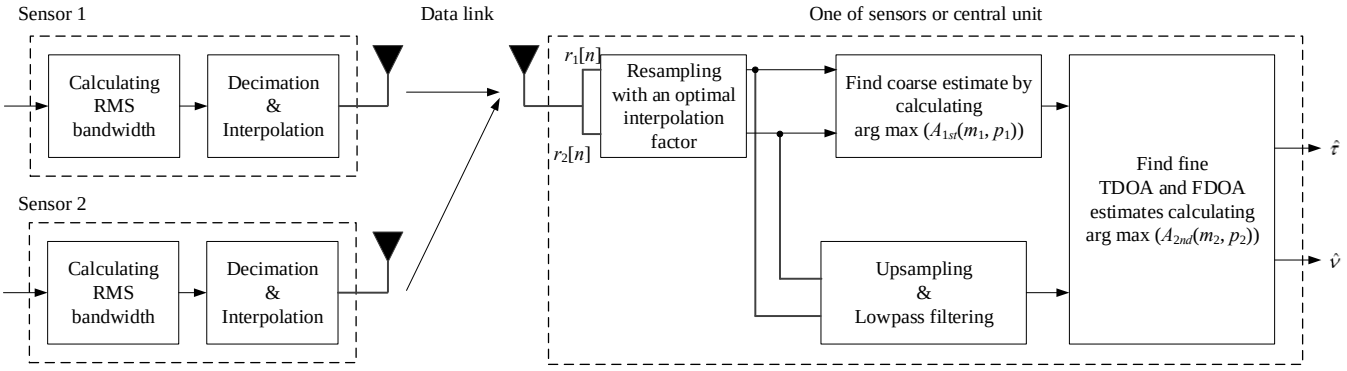

Fig. 3. Block diagram of two stage algorithm using optimal interpolation factor.

After the optimal interpolation factor M_2 is determined, the sampling rate of transferred data is changed into f_{s2}/M_2 by using a resampling block composed of interpolation and decimation. Coarse estimates can be obtained by m_1 and p_1, where the maximum value of the modified CAF function (3) based on the resampled signal appears. The CAF in (3) can be implemented using FFT with length Q_1 resulting from K_1 summed values of L_1 samples by (4) and $(Q_1–K_1)$ zeros by zero padding, as explained in Section II. The frequency-domain sampling interval (FDSI) without zero padding is $1/T$, which depends on only the collection time. Thus, in the EW system, the FDSI is more than several hertz in a usual situation where the collection time is under one second. So, we need zero padding to achieve the target FDSI.

In the second stage, interpolation for fine TDOA/FDOA estimates is carried out, and coarse estimates acquired from the first stage are used to consider only a narrow region near these coarse estimates. Firstly, $r_1[n]$ and $r_2[n]$ are extended by inserting M_2-1 zeros between consecutive samples in $r_1[n]$ and $r_2[n]$, respectively. Then, the interpolated sequences of $d_1[n]$ and $d_2[n]$ are obtained by low-pass filtering of the extended sequences. So, the time resolution of $d_1[n]$ and $d_2[n]$ is enhanced by M_2 times compared to the first stage. Consequently, the interpolated sequences of $d_1[n]$ and $d_2[n]$ are inserted into the second stage for computing fine CAF as follows:

$$A(m_2, p_2) = \sum_{n=0}^{N_2-1} d_1[n] d_2^*[n+m_2] \exp\left(-j2\pi \frac{p_2 n}{N_2}\right), \quad (21)$$

$$\text{for} \quad \hat{\tau}_1 - \frac{M_2}{2} \le m_2 < \hat{\tau}_1 + \frac{M_2}{2}, \ \hat{\nu}_1 - \frac{P_2}{2} \le p_2 < \hat{\nu}_1 + \frac{P_2}{2}$$

where only P_2 points are calculated using a pruned FFT to reduce the computational burden. Also, the number of points Q_2 for FFT in the second stage is related to Q_1 samples in the first stage as follows:

$$Q_2 = kQ_1, \quad k = r_2 / r_1, \quad k: \text{positive integer} \quad (22)$$

The reason why Q_2 is a multiple of Q_1 is that the grid in the second stage must include the points corresponding to the coarse estimates. Thus, in the second stage, the number of increased samples between each sample in the second stage is k such that P_2 is determined as $2k$-1. Fig. 3 illustrates the overall process of the proposed algorithm.

IV. Numerical Evaluation

To verify the efficiency of the proposed algorithm, its computational complexity was compared with that of methods with a non-optimal interpolation factor through computer simulations using various parameters. Also, its root mean-square error (RMSE) was compared with the corresponding Cramer-Rao lower bound (CRLB) of TDOA and FDOA for theoretical analysis. For numerical evaluation, we used a sampling frequency of f_s=100 MHz, collection time of T=0.1s, difference between minimum and maximum FDOAs of v_D=6.8 kHz, time resolution of $1/f_{s2}$=10 ns, frequency-domain sampling interval of v_o=1 Hz, noise bandwidth of $B=f_{s2}/M_2$, and distance between each sensor of R=20 km. From these parameters, the parameter of M related to the TDOA range of interest was determined as 6,671 from (9).

Transmitted symbols are pulse-shaped with a raised cosine pulse, and the radiated signal of an unknown emitter is given by [22]:

$$s(t) = \sum_{i=0}^{I-1} a_i \frac{\sin(\pi(t-iT_t)/T_t)}{\pi(t-iT_t)/T_t} \frac{\cos(\pi\beta_r(t-iT_t)/T_t)}{1-(2\pi(t-iT_t)/T_t)^2}, \quad (23)$$

where T_t is the symbol duration, which was 25 μs, β_r is the roll-off factor, which was assigned by 0.8, and a_i are randomly generated symbols from the set A chosen by a modulation method. In this experiment, BPSK (A = {±1}), QPSK (A = {±1, ±j}) and 16-QAM (A = {±1±j, ±3±j, ±1±3j, ±3±3j}) are used to adjust various modulation methods. The power or the variance of additive noise is determined by:

$$\sigma_n^2 = P_s \times 10^{-SNR_{\text{dB}}/10}, \quad (24)$$

where SNR_{dB} is the given SNR in dB, and P_s is the signal power defined by:

This article has been accepted for publication in a future issue of this journal, but has not been fully edited. Content may change prior to final publication. Citation information: DOI 10.1109/TAES.2017.2735118, IEEE Transactions on Aerospace and Electronic Systems

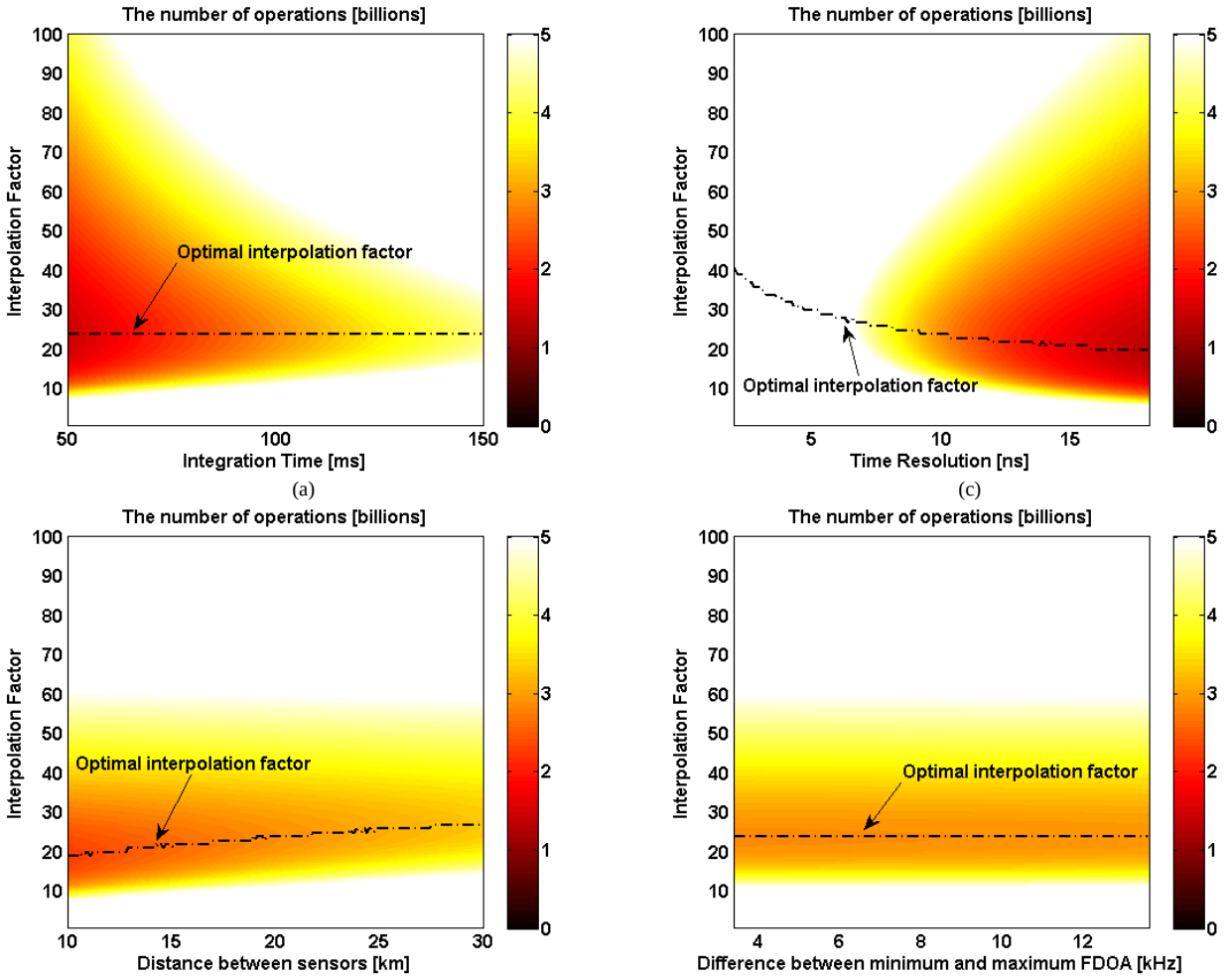

Figure 4. The number of operations according to the interpolation factor in each circumstance that control parameters change: (a) collection Time, (b) distance between sensors, (c) time resolution, (d) maximum velocity.

$$P_s = \frac{1}{N_1}\sum_{n=0}^{N_1}\left|s(n)\right|^2, \tag{25}$$

Here, $s(n)$ is the sampled signal from $s(t)$ with a sampling frequency of f_s.

A. Computational complexity

Figure 4 shows the number of operations versus interpolation factors varying with the control parameters, such as (a) the collection time, (b) the distance between sensors, (c) the time resolution, and (d) the maximum velocity related to the difference between the minimum and maximum FDOAs. We marked the optimal interpolation factor corresponding to the minimum operations with a line in each figure. In the dark region, we can analyze how much the control parameters affect the number of operations. As shown in Fig. 4, the number of operations decreases as the collection time, time resolution, and between the sensors are reduced. On the other hand, the difference between the minimum and maximum FDOAs hardly affect the number of operations. Also, the computational load of each stage according to the control parameters can be found from the tendency of the optimal interpolation factor lines appearing in each plot.

In Figs. 4(a) and (d), the optimal interpolation factors remain constant, irrespective of the change of the control parameters. This means that the computational complexity of each stage increases or decreases with an equal ratio as the collection time and the difference between the minimum and the maximum FDOAs vary. In Figs. 4(b) and (c), the optimal interpolation factor lines are curve shaped because the computational complexities of the first and second stages increase simultaneously, but more so in the first stage when the time resolution and distance between sensors increase.

The strength of the proposed algorithm lies in the computational efficiency from adding a resampling block related to the optimal interpolation factor when the received signal is unknown. To verify this, we define an efficiency factor:

$$\zeta = 1 - \frac{NC \text{ using an optimal interpolation factor}}{NC \text{ using a non-optimal interpolation factor}}. \tag{26}$$

This article has been accepted for publication in a future issue of this journal, but has not been fully edited. Content may change prior to final publication. Citation information: DOI 10.1109/TAES.2017.2735118, IEEE Transactions on Aerospace and Electronic Systems

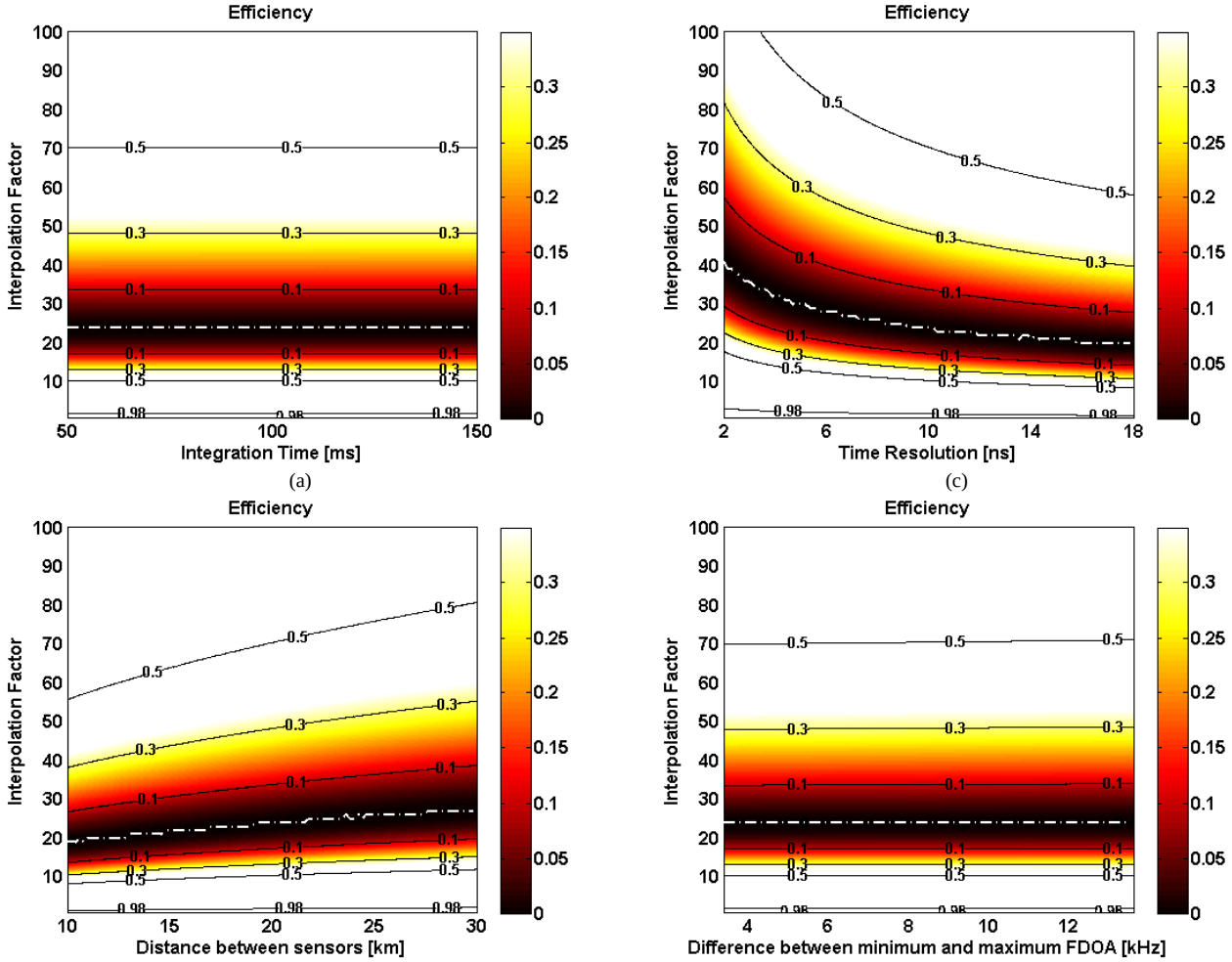

Figure 5. Efficiency factor according to the interpolation factor in each circumstance that the control parameters change: (a) collection Time, (b) distance between sensors, (c) time resolution, (d) maximum velocity.

Fig. 5 shows how the efficiency factors vary according to the interpolation factors under variation of the control parameters. We marked the optimal interpolation factors with a dash-dot white line in each figure. When the interpolation factor is set to one, the interpolation process is not performed. Thus, the number of operations is almost identical to that of Stein's algorithm except for a single FFT operation required to find a fine FDOA in the second stage. As a result, the computational complexity can be reduced more than 98% by using the proposed method compared with Stein's algorithm, as shown in Fig. 5.

In the case of the conventional two-stage method, the interpolation factor is determined by the sampling frequency when the final resolution is fixed. Thus, this interpolation factor may not be optimal, resulting in higher computational complexity than that of the proposed algorithm, as shown in Fig. 5. On the other hand, the computational complexity of the conventional two-stage method may be the same as that of the proposed method when the optimal interpolation factor is used. However, the datalink time of the two-stage method is too long to adjust the emitter localization system in EW due to the absence of a resampling block.

The efficiency factor is presented in Fig. 6 using different y-axis ranges under the same conditions as Fig. 5. This data show for comparison of the computational efficiency between the proposed algorithm and the conventional two-stage algorithm when the datalink time is the shortest while satisfying the Nyquist sampling theorem. In this simulation, the bandwidth of the received signal is set as 40 kHz, so the sampling frequency can be set as 50 kHz with a margin. If the final time resolution is set as 10 ns, the interpolation factor is 2,000. Fig. 6 shows that the proposed algorithm is more than 97% efficient compared to the conventional two-stage method.

B. Estimation accuracy

We verified the estimation accuracy of the proposed algorithm by using simulation results in two ways. In the first approach, the estimation accuracy of the proposed algorithm is presented in realistic EW circumstances using parameters described in the first paragraph of Section IV. In the second approach, the precision of the proposed algorithm using a resampling block is compared with that of Stein's method and the two-stage method using a non-optimal interpolation factor. However, these conventional methods are hard to simulate

This article has been accepted for publication in a future issue of this journal, but has not been fully edited. Content may change prior to final publication. Citation information: DOI 10.1109/TAES.2017.2735118, IEEE Transactions on Aerospace and Electronic Systems

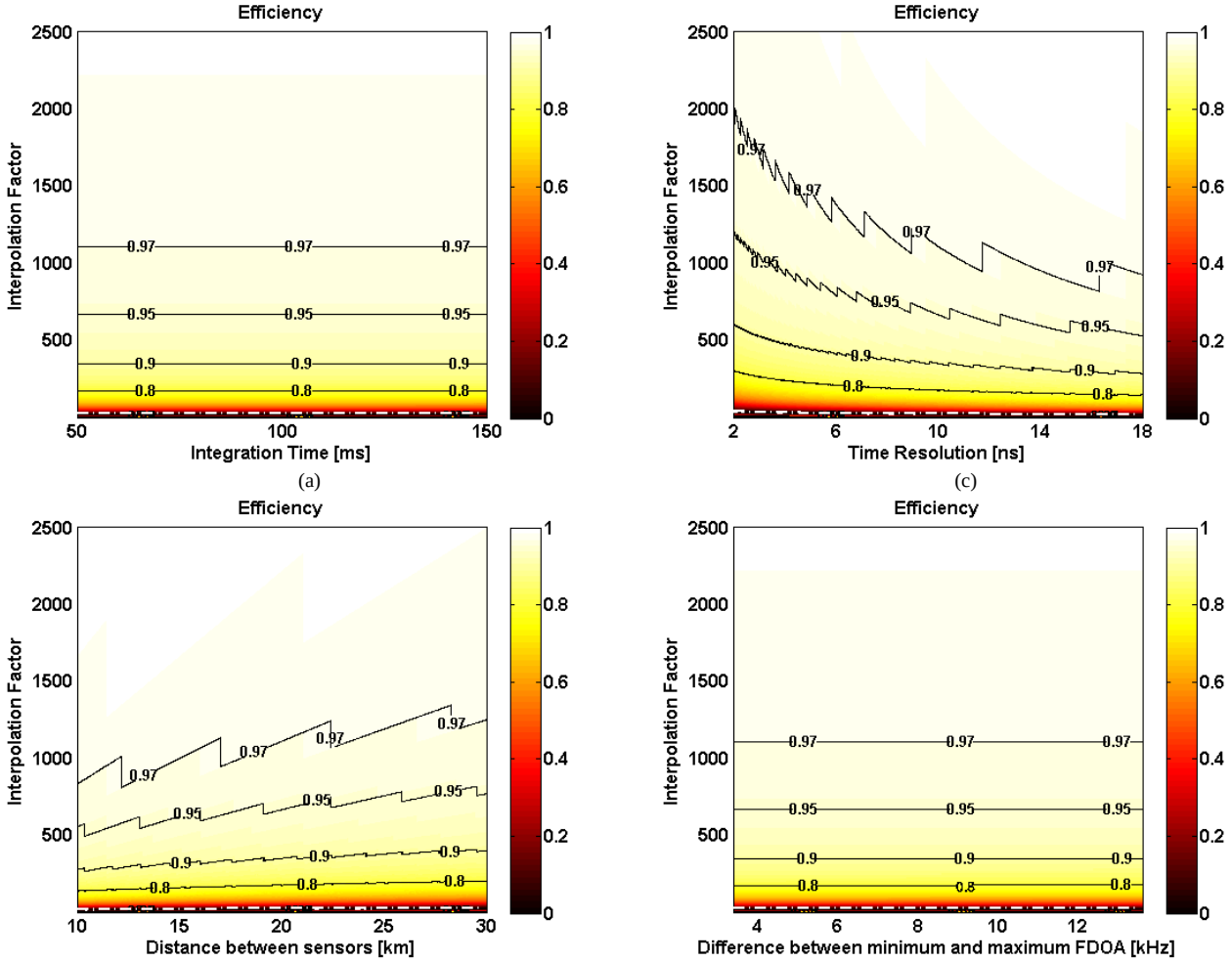

Figure 6. Efficiency factor according to the interpolation factor from 1 to 2500 in each circumstance that the control parameters change: (a) collection Time, (b) distance between sensors, (c) time resolution, (d) maximum velocity.

under EW circumstances due to their enormous computational complexity. Thus, we used reasonable parameters to reduce the simulation burden for this comparison.

Fig. 7 shows the RMSE for TDOA and FDOA of the proposed algorithm and CRLB with various symbol rates. We used BPSK, 4-PSK, and 16-QAM signals. From the results of 200 independent trials, the RMSEs for TDOA and FDOA were calculated by:

$$\begin{aligned} \mathrm{RMSE}_{\tau} &= \left(\frac{1}{200} \sum_{l=1}^{200} \left(\hat{\tau}_d(l) - \tau_d(l) \right)^2 \right)^{1/2}, \\ \mathrm{RMSE}_{\nu} &= \left(\frac{1}{200} \sum_{l=1}^{200} \left(\hat{\nu}_d(l) - \nu_d(l) \right)^2 \right)^{1/2}, \end{aligned} \tag{27}$$

where l is the trial number.

CRLB represents the lower bound on the variance of estimators and was used for theoretical analysis. Those of TDOA and FDOA estimates were derived in previous studies as follows [14, 20]:

$$\mathrm{var}(\hat{\tau}_d) \geq \frac{1}{4\pi^2 B T \gamma B_{rms}^2}, \quad B_{rms} = \sqrt{\frac{\int_{BW} f^2 |S(f)|^2 \, df}{\int_{BW} |S(f)|^2 \, df}} \tag{28}$$

$$\mathrm{var}(\hat{\nu}_d) \geq \frac{1}{4\pi^2 B T \gamma T_e^2}, \quad T_e = \sqrt{\frac{\int_0^T t^2 |s(t)|^2 \, dt}{\int_0^T |s(t)|^2 \, dt}} \tag{29}$$

where B is the noise bandwidth and γ is the effective SNR defined by:

$$\frac{1}{\gamma} = \frac{1}{2} \left[\frac{1}{\gamma_1} + \frac{1}{\gamma_2} + \frac{1}{\gamma_1 \gamma_2} \right]. \tag{30}$$

Here, γ_1 and γ_2 are SNRs at Sensor 1 and Sensor 2, respectively.

As shown in Figs. 7(a) and (c), the TDOA performance of the estimator degrades as the symbol rate decreases. This tendency matches well with the theoretical CRLB performance of (28). Also, the performance of the proposed algorithm approaches the CRLB as SNR increases.

This article has been accepted for publication in a future issue of this journal, but has not been fully edited. Content may change prior to final publication. Citation information: DOI 10.1109/TAES.2017.2735118, IEEE Transactions on Aerospace and Electronic Systems

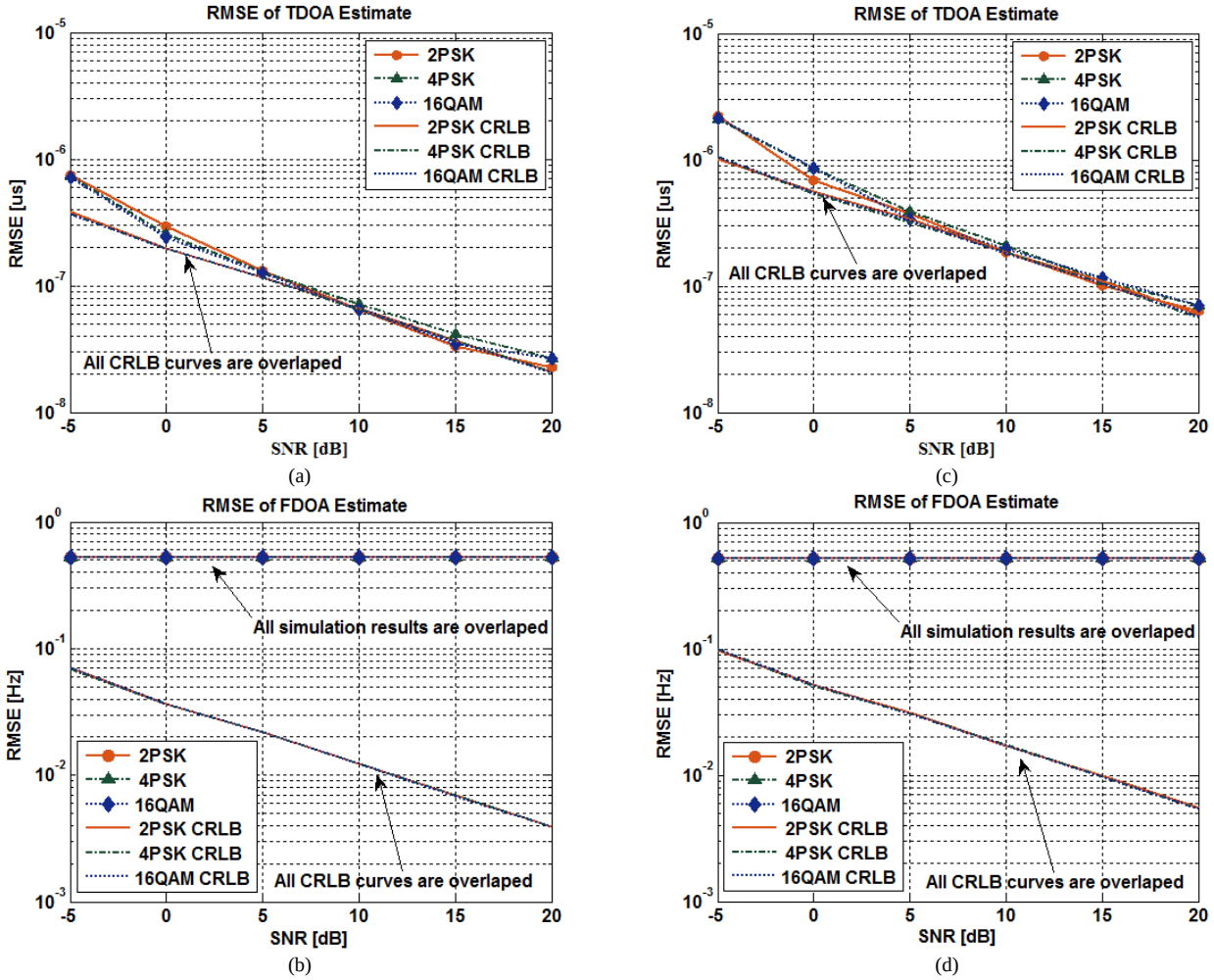

Figure 7. RMSEs of TDOA and FDOA estimates and CRLBs according to the symbol rates of (a) TDOA 40 kHz, (b) FDOA 40 kHz, (c) TDOA 20 kHz, (d) FDOA 20 kHz.

Figs. 7(b) and (d) show the RMSEs and the CRLBs for the FDOA estimates of the proposed method under the same conditions. Generally, the FDOA performance of communication signals is better than that of radar signals [1]. Thus, if considering a communication signal, there can be a margin in reducing the number of operations for FDOA rather than TDOA, despite the possibility of degradation in the estimation accuracy. In this sense, even though the target resolution at frequency v_o is lower than the theoretical CRLB performance for the overall SNR, it was set as 1 Hz so that the RMSE for FDOA has a constant value of about 0.5 Hz with varying SNR, as in Figs. 7(b) and (d). The estimation accuracy of 1 Hz or smaller for FDOA is known to be sufficient for emitter localization in EW [4].

Fig. 8 shows the RMSEs for TDOA and FDOA of the proposed algorithm and those of the conventional algorithms, respectively. For this comparison, we used tractable parameters to reduce the number of overall operations instead of the realistic parameters used to verify the estimation accuracy of the proposed method. The values used were a sampling frequency of f_s=100 kHz, collection time of T=5 ms, time resolution of $1/f_{s2}$=200 ns, and distance between each sensor of R=5 km.

As shown in Fig. 8(a), the TDOA performance of the proposed algorithm is almost the same as that of the two-stage algorithm using a non-optimal interpolation factor and Stein's algorithm. Similarly, in Fig. 8(b), the FDOA performance of the proposed algorithm did not degrade compared with the conventional algorithms. The simulation results show that the proposed method maintains performance with much less computational complexity compared with the conventional methods.

V. Conclusion

We have presented a computationally efficient TDOA/FDOA estimation algorithm by adding a resampling block to reduce the number of operations and time for the datalink between sensors when the bandwidth of a received signal is completely unknown. The proposed method accomplishes this goal while maintaining estimation accuracy compared with conventional methods by using the resampling block with an optimal interpolation factor for different control parameters such as the distance between sensors and collection time. Also, we introduced an efficiency factor to verify the efficiency of the proposed algorithm. The suggested algorithm

This article has been accepted for publication in a future issue of this journal, but has not been fully edited. Content may change prior to final publication. Citation information: DOI 10.1109/TAES.2017.2735118, IEEE Transactions on Aerospace and Electronic Systems

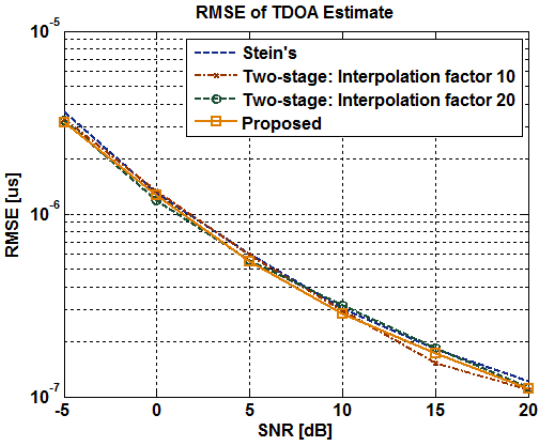

(a)

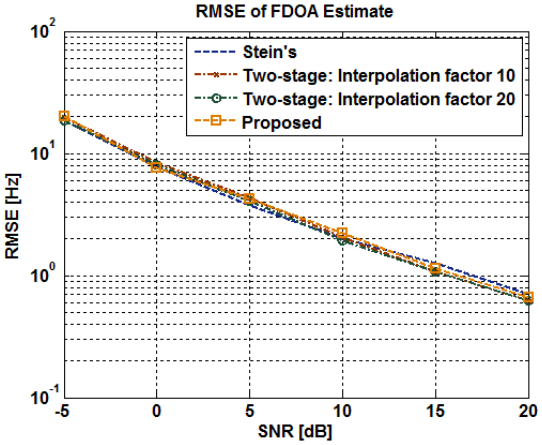

(b)

Figure 8. RMSEs of estimates according to the proposed algorithm and the conventional method: (a) TDOA, (b) FDOA.

can be applicable for systems that require high-speed processing to estimate the position of an unknown emitter.

REFERENCES

[1] Paradowski, L. R. "Microwave emitter position location: present and future," *in Proc. Microwaves and Radar*, vol4, pp. 97-116, 1998.

[2] Adamy, D. L. EW 103: Tactical Battlefield Communications Electronic Warfare, Artech House, 2001.

[3] Chan, Y. T., and Ho, K. C. "A simple and efficient estimator for hyperbolic location," *IEEE Trans. Signal Process.*, vol. 42, no. 8, Aug. 1994.

[4] Ho, K. C. "An accurate algebraic solution for moving source location using TDOA and FDOA measurements," *IEEE Trans. Signal Process.*, vol. 52, no. 9, pp. 2453-2463, Sep. 2004.

[5] Yoon, J.-Y., Kim, J.-W., Lee, W.-Y., and Eom, D.-S. "A TDOA-based localization using precise time-synchronization," *14th International Conference on Advanced Communication Technology*, pp. 1266-1271, Feb. 2012.

[6] Stein, S. "Differential delay/Doppler ML estimation with unknown signals," *IEEE Trans. Signal Process.*, vol. 41, no. 8, pp. 2717-2719, Jun. 1993.

[7] Shin, D. C., and Nikias, C. L. "Complex ambiguity functions using nonstationary higher order cumulant estimates," *IEEE Trans. Signal Process.*, vol. 43, no. 11, pp. 2649–2664, Nov. 1995.

[8] Ulman, R., and Geraniotis, E. "Wideband TDOA/FDOA processing using summation of short-time CAF's," *IEEE Trans. Signal Process.*, vol. 47, no. 12, pp. 3193–3200, Dec. 1999.

[9] Yeredor, A., and Angel, E. "Joint TDOA and FDOA estimation: a conditional bound and its use for optimally weighted localization," *IEEE Trans. Signal Process.*, vol. 59, no.4, Apr. 2011.

[10] Hartwell, G. D. "Improved geo-spatial resolution using a modified approach to the complex ambiguity function", M. S. thesis, Naval Postgraduate School, 2005.

[11] Hu, X. "Computing the Cross Ambiguity Function," M. S. thesis, Dept. Electrical Engineering, Binghamton Univ., New York, 2005.

[12] Tao, R., Zhang, W.-Q., and Chen, E.-Q. "Two-stage method for joint time delay and Doppler shift estimation," *IET Radar Sonar Navig.*, vol. 2, no 1. pp. 71-77, Jan. 2008.

[13] Johnson, J. J. "Implementing the cross ambiguity function and generating geometry-specific signals," M. S. thesis, Dept. Electrical Engineering, Naval Postgraduate School, Monterey, Sep. 2001.

[14] Stein, S. "Algorithm for Ambiguity Function Processing," *IEEE Trans. Acoust., Speech, Signal Process.*, vol. ASSP-29, no. 3, pp. 588-599, Aug. 1981.

[15] Chen, M., and Fowler, M. L. "Data compression for multi-parameter estimation for emitter location," *IEEE Trans. Aerosp. Elect. Sys.*, vol. 46, pp. 308–322, Jan. 2010.

[16] Gai, J., Chan, F., Chan, Y. T., Du, H., and Dikes, F. A. "Frequency estimation of uncooperative coherent pulse radars," *in Proc. IEEE Military communications conference*, 2007, pp. 1-7. Oct. 2007.

[17] Pourhomayoun, M., and Fowler, M. L. "Cramer-Rao bound for frequency estimation in coherent pulse train with unknown pulses," *IEEE Trans. Aerospace and Electronic Systems*, vol. 50, no. 2, Apr. 2014.

[18] Skinner, D. P. "Pruning the decimation in-time FFT algorithm," *IEEE Trans. Acoust., Speech, Signal Process.* vol. 24, no. 2, pp. 193-194, Apr. 1976.

[19] Kay, S. Fundamentals of Statistical Signal Processing, Volume 1, Estimation Theory, Englewood Cliffs, NJ: Prentice Hall, 1993.

[20] Panek, P. "Error analysis and bounds in time delay estimation," *IEEE Trans. Signal Process.*, vol. 55, no.7, pp. 3547-3549, Jul. 2007.

[21] Kim, D.-G., Kim, Y.-H., Song, K.-H., Han, J.-W., and Kim, H.-N. "Analysis on the effect of geometric deployment and velocities of sensors based on TDOA/FDOA measurements," *in proc. IASTED Int. Conf. Signal Processing, Pattern Recognition and Applications (SPPRA'2013)*, Innsbruck, Austria, Feb. 2013.

[22] Proakis, J. G., and Salehi, M. Digital Communications, McGRAW-Hill, 2007.